Int J Earth Sci (Geol Rundsch)
DOI 10.1007/s00531-009-0429-1

ORIGINAL PAPER

Morphobathymetric analysis and evidence of submarine mass movements in the western Gulf of Taranto (Calabria margin, Ionian Sea)

M. Rebesco · R. C. Neagu · A. Cuppari · F. Muto · D. Accettella · R. Dominici · A. Cova · C. Romano · A. Caburlotto

Received: 20 July 2007 / Accepted: 8 February 2009

Abstract The western part of the Gulf of Taranto, southern Italy, is a seismically active area with high sediment supply. New swath bathymetry and sub-bottom profiler (CHIRP) data were acquired on board R/V OGS-Explora during the WGDT cruise. The data were analyzed to describe the seafloor morphology and the acoustic facies of relevant morphologic features. Special attention was given to the features produced by mass wasting and soft-sediment deformations. The features identified include: slides and slide scars, debris flow deposits, enigmatic dip-slope trending sub-parallel linear depressions, and along-slope undulations inferred to have been produced either by creeping or sediment deposition by hyperpycnal flows. The description of these features contributes to the characterization of the Calabria foreland basin system and provides an analogue for other basins similarly affected by a close relation between sediment supply and active tectonics.

M. Rebesco · R. C. Neagu · D. Accettella · A. Cova · A. Caburlotto
Istituto Nazionale di Oceanografia e di Geofisica Sperimentale (OGS), Borgo Grotta Gigante 42/C, Sgonico, 34010 Trieste, Italy

R. C. Neagu (✉)
3D Lab, School of Earth and Ocean Sciences, Cardiff University, Main Building, Park Place, Cardiff CF10 3YE, UK
e-mail: ralukaneagu@gmail.com

A. Cuppari
Dipartimento di Scienze Geologiche Ambientali e Marine, Università degli Studi di Trieste, Via E. Weiss 2, 34127 Trieste, Italy

F. Muto · R. Dominici · C. Romano
Dipartimento di Scienze della Terra, Università degli Studi della Calabria, 87036 Arcavacata di Rende (CS), Italy

Keywords Gulf of Taranto · Morphobathymetry · Sub-bottom profiling · Mass movements

Introduction

The exploration of the seafloor during the last three decades by means of high-resolution swath bathymetry and sub-bottom profiling has illustrated the widespread occurrence of submarine instabilities. In consequence, and due to its multiple implications, the characterization and understanding of mass wasting phenomena on continental margins has become a priority topic (e.g. Canals et al. 2004 and references therein). Tens to hundreds of meters in thickness soft-sediment deformation generated by tectonism, rapid deposition and/or compaction and fluid flow has emerged as a highly relevant process in the evolution of sedimentary basins. The analysis of deformation features may allow a better understanding of the temporal and spatial evolution of the basins and the post-depositional geometry of subsurface hydrocarbon reservoirs. Moreover, mass wasting actively contributing to the shaping of the continental slope can affect both onshore and offshore infrastructures. Thus, a better understanding of these processes is crucial in planning and managing human activities in offshore regions.

Instabilities and deformation features of variable thicknesses and types, including creeping, slides, slumps and mass flows, were first recognized in the northern Gulf of Taranto (Rossi and Gabbianelli 1978) and especially in the Corigliano Basin (Romagnoli and Gabbianelli 1990 and references therein). Among the several interplaying factors contributing to the widespread instability, a prominent role was attributed to high depositional input and subsequent under consolidation state of the deposits, the presence of

Published online: 27 February 2009

diffuse gas within the sediments, and recent tectonic activity (Romagnoli and Gabbianelli 1990).

The first aim of this paper is presenting new swath bathymetry data and sub-bottom profiles to describe the seafloor morphology of the western Gulf of Taranto. Secondly, we use the morphological expression and the internal structure of sediment units affected by mass movements to infer the factors and triggering mechanisms involved in slope destabilisation.

Regional setting: morphology and geology

The Gulf of Taranto is located offshore southern Italy in the northwestern part of the Ionian Sea, between Calabria and Puglia (Fig. 1). The centrally located Taranto Valley is considered the modern foreland basin of the southern Italian orogenic system, with the autochthonous foreland platform to the east and the southeastern extremity of the allochthonous thrust sheets of the southern Apennine Chain and Calabrian-Peloritain Arc to the west (Boccaletti et al. 1984; Rossi and Sartori 1981; Senatore et al. 1988; Critelli and Le Pera 1998; Critelli 1999 among others). Compressional tectonics has played a key role in shaping the structure of the Gulf as emphasized by several authors (Finetti 1976; Pescatore and Senatore 1986, Senatore 1987; Senatore et al. 1988; Del Ben 1993). Others have highlighted the role of gravitational deformation by normal faulting (Rossi et al. 1983).

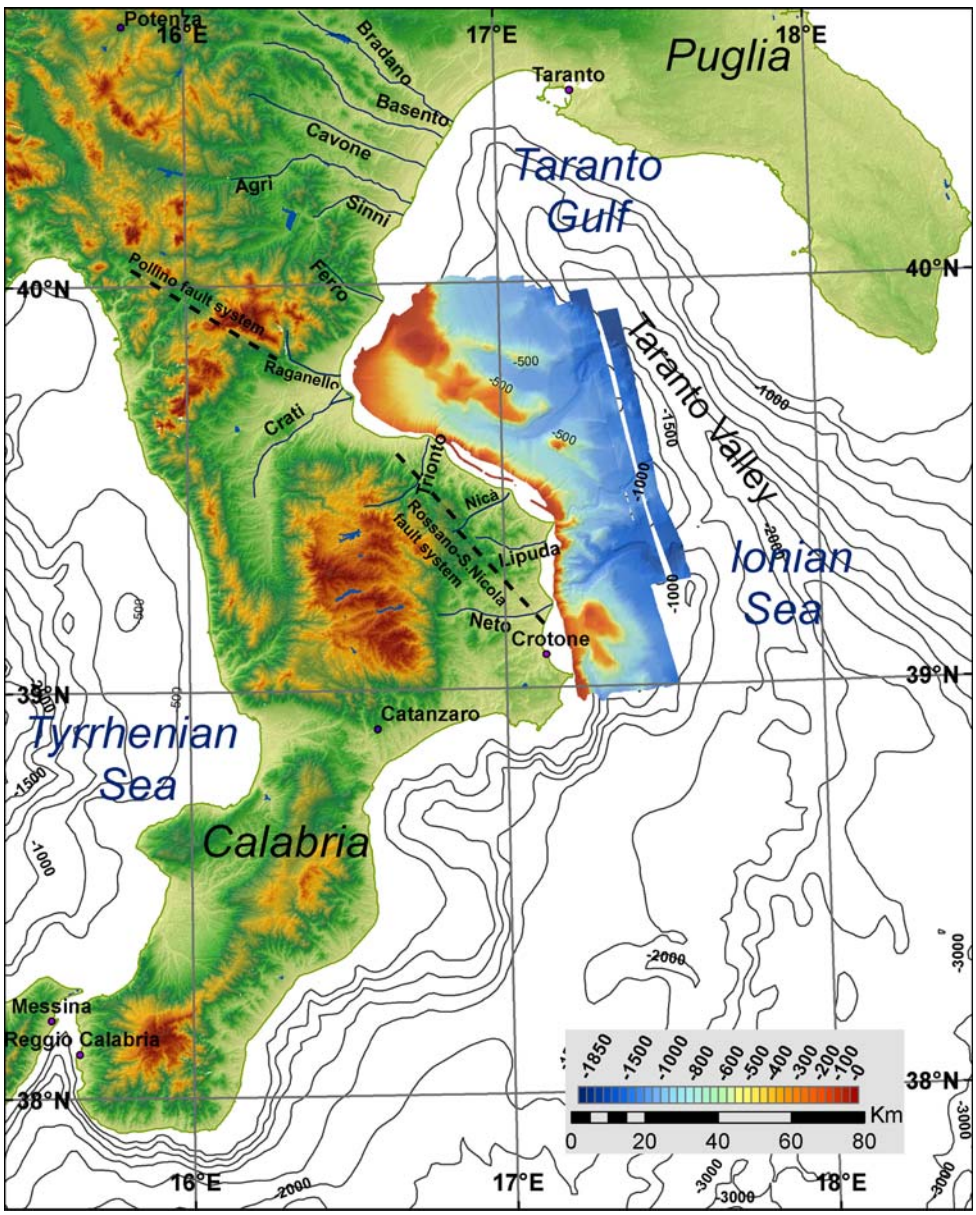

Fig. 1 General sketch map of the investigated area in the Gulf of Taranto. Contour interval = 250 m. The position of the mouths of the main rivers along the coasts of the northwestern Gulf of Taranto, and of the Rossano-S. Nicola and Pollino fault systems are also shown

Calabrian fold systems, thrusts and high angle faults continue offshore where they have been partly explored by oil companies (Doglioni et al. 1999; Van Dijk et al. 2000). Folds and positive flower structures are associated to the propagation of thrusts. The main fault system is represented by the NW–SE trending sinistral transpressive Rossano-S. Nicola (Van Dijk et al. 2000), and the Pollino fault zones (Bousquet 1973; Ferranti et al. 2008). Minor splays of these transcurrent and transpressive systems involve the basin margins and are arranged in *en-echelon* often representing the conjugate faults of the main structures.

The western Gulf of Taranto, which belongs to the Calabrian margin, displays a complex morphology that consists of ridges and basins related to the Neogene-quaternary geodynamic evolution of the submerged, tectonically active extremity of the southern Apennines (Romagnoli and Gabbianelli 1990). Its structural evolution has been determined mainly by extensional NW–SE and, to a lesser extent, NE–SW trending regional faults (Romagnoli and Gabbianelli 1990). At the northernmost part of the study area, and from west to east, the main morphotectonic features are the Corigliano Basin, the Amendolara ridge and the Amendolara Basin (Fig. 2). Both Corigliano and Amendolara basins are neotectonic depressions developed close to the NW-SE trending sinistral strike-slip shear zone (Pollino fault system) at the boundary between the Apennine Chain and the Calabrian-Peloritain Arc. They have been interpreted as piggy-back basins behind a thrust sheet (Pescatore and Senatore 1986; Senatore 1987) and also as part of the wide wedge-top depozone (DeCelles and Giles 1996) of the modern southern Italy foreland basin system (Critelli and Le Pera 1998; Critelli 1999).

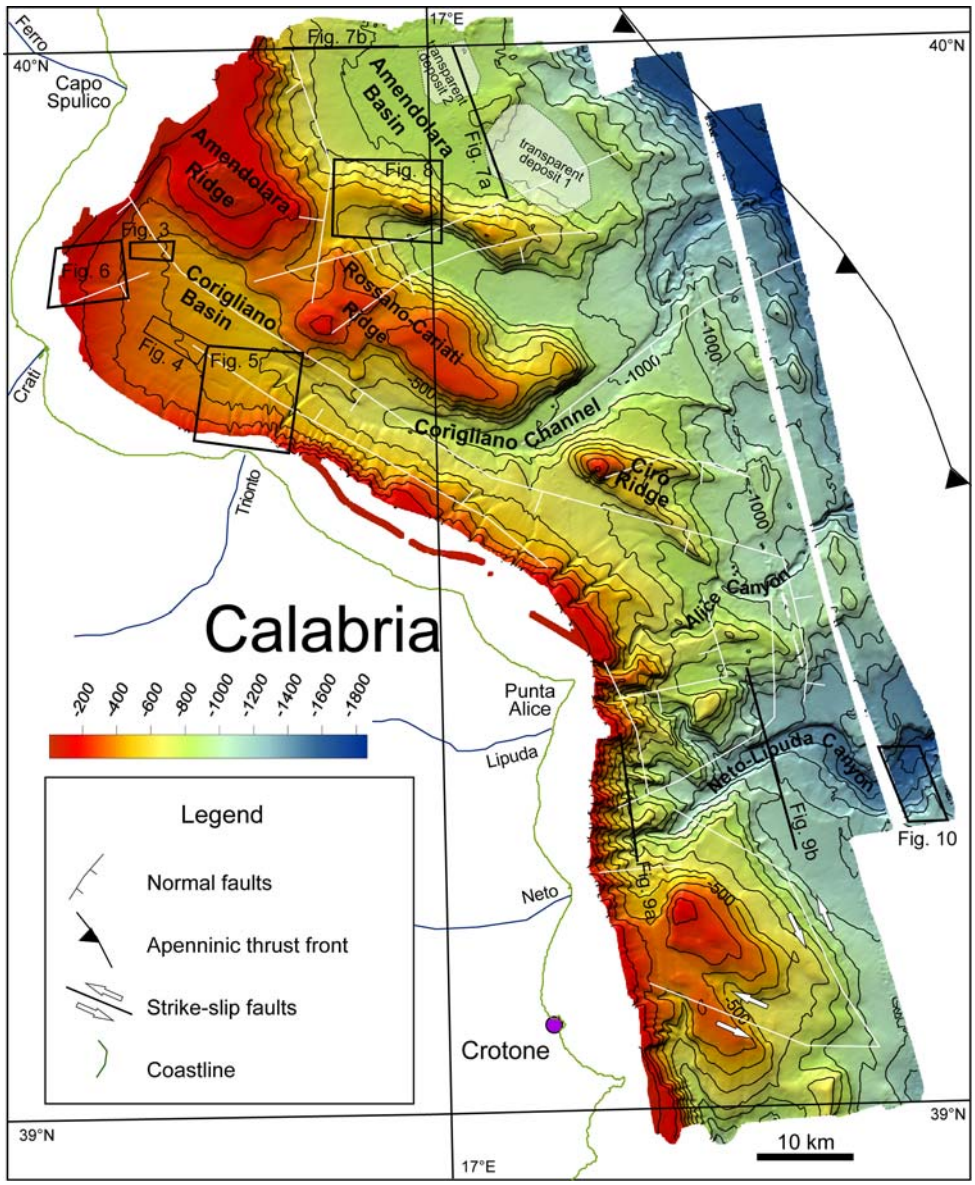

Fig. 2 *Shaded* relief multibeam bathymetry of the southwestern part of the Gulf of Taranto with location of the figures. Grid spacing = 50 m; vertical factor = 3; illumination from 340°; contour interval = 100 m. Faults (*in white*) are modified from Boccaletti et al. 1984

The NW–SE elongated Corigliano Basin is nearly 60 km long, less than 20 km wide, and about 200–800 m deep (Fig. 2). It is flanked by the northern Calabria continental slope to the SW and by the ~200 m deep Amendolara and Rossano-Cariati structural ridges to the NE. The Corigliano Basin includes a narrow shelf reaching its maximum width (up to 6 km) in its northern part and narrowing down to less than 1 km in its southern part. This basin is sediment supplied mainly by the Crati River (Romagnoli and Gabbianelli 1990; Fig. 1), which carries a tremendous load (1,730,000 t/yr) to the sea, most of which as suspended sediment. Recent sedimentation rates in the Corigliano Basin are as high as 6 mm/year (Ricci Lucchi et al. 1984). The southwestern shelf and upper slope of the Corigliano Basin are cut by numerous gullies, most of them connected to the Crati and Trionto rivers (Fig. 1). These gullies are active and transport terrigenous material downslope towards the Corigliano Channel, which in turn feeds the large Taranto Valley to the east (Rossi and Gabbianelli 1978; Romagnoli and Gabbianelli 1990; Figs. 1, 2).

A few meters thick marker horizon made of three relatively high-amplitude sub-parallel reflectors, named "R horizon" by Romagnoli and Gabbianelli (1990), has been identified within the sediment infill of the Corigliano Basin. These authors inferred that the sediments at the R horizon are slightly coarser than the underlying and overlying ones and attributed this to stream rejuvenation induced by tectonic uplift or the Younger Dryas(?) climatic shift at the late Pleistocene–Holocene transition. Some peculiar acoustic features in sub-bottom profiles above the R horizon (Pleistocene–Holocene) have been interpreted as the product of soft-sediment deformation including creep folds and pockmarks (Romagnoli and Gabbianelli 1990).

Westward of the Corigliano Basin, the Amendolara Ridge represents the south-eastward prolongation of an onshore ridge and is bounded both towards the east and towards the coast by faults exhibiting modest dip-slip components (Senatore et al. 1988; Figs. 1, 2).

On the middle continental slope east of Amendolara Ridge, the flat-bottomed, roughly NW–SE elongated Amendolara Basin (Fig. 2) constitutes the submerged extension of an onshore neotectonic graben (Rossi et al. 1983). The Amendolara and the Rossano-Cariati ridges that are less than 200 m deep separate the Amendolara Basin from the Corigliano Basin. The lower part of the Amendolara Basin, which is suspended above the deep Taranto Valley, is over 1,000 m deep. The Amendolara Basin is supplied by the Sinni and Agri rivers and by numerous torrential streams that experience frequent flash floods (Romagnoli and Gabbianelli 1990). The prograding shelf width varies between 9 and 14 km and shows an average gradient of 1° (Pescatore and Senatore 1986).

South of the Corigliano Channel, the shelf is very narrow, its width ranging from a few kilometers to less than 1 km. Numerous canyons and gullies cut the shelf and upper slope, the largest being the Neto-Lipuda Canyon offshore the Neto River mouth (Pennetta 1992; Figs. 1, 2).

Data set

The data presented in this paper were acquired by the R/V OGS-Explora during the western Gulf of Taranto (WGDT) cruise (August 21st–September 1st, 2005). Swath-bathymetry and sub-bottom profiler (CHIRP) data were acquired simultaneously.

For Swath-bathymetry two hull-mounted Reson SeaBat multibeam echosounder systems were used, the 8111 system down to about 500 m depth and the 8,150 system for larger depths. The SeaBat 8111, operating at a frequency of 100 kHz, reaches the maximum swath width (7.5 times the water depth) when working in less than 150 m of water. The 8111 system illuminates a swath on the sea floor that is 150° across track by 1.5° along track. The maximum selectable range scale is 1,400 m. The swath consists of 101 individual 1.5° by 1.5° beams with a bottom detection range resolution of 3.7 cm. The 8111 system employs pitch stabilization to steer the transmitted beam so that it remains vertical through pitch angles of ±10°. The SeaBat 8150, operating at a frequency of 12 kHz, is a full ocean depth multibeam echo sounder system. The maximum selectable range scale is 15,000 m; however, maximum swath width is typically achieved at water depths of approximately 6,000 m. The 8150 system forms 234 receiver beams across a sector up to 150° wide. The 8150 sonar processing unit performs initial signal processing, time delay beam forming, and bottom detection. The beamforming process is equi-angular. The 8150 employs both pitch and active roll compensation to steer the receiver beams so that the nadir beam remains vertical through roll angles of ±10°.

Pitch, roll, heave and heading values are provided by the Inertial Navigation System IXSEA PHINS. Continuous velocity values used to perform the dynamic beam steering are provided by the keel mounted Navitronic SVP71 sound velocity probe. The data are acquired and stored by the navigation software PDS2000.

For the sub-bottom profiler data a Benthos CAP-6600 profiler was utilized. It consists of 16 keel mounted AT 471 transducers and a top side unit, composed of an analogic amplifier and a data logger. A 16 bits DSP card performs the analogic/digital conversion. Sweeps range between 2 and 7 kHz. Communication Technology SwanPro acquisition software was used to collect the data, which were acquired in XTF format and subsequently stored either in XTF and SEG Y format. The depth in the sub-bottom

profiles shown in this paper is indicated in time (milliseconds). A constant sound velocity of 1,500 m/s has been assumed to calculate sub-bottom depths and thicknesses in meters.

Swath bathymetry data covering an area of 5,100 km^2 were processed at OGS using the Reson PDS2000 V 2.5.3.2 software. Editing steps included: (1) application of calibration parameters (time-pitch-roll-yaw) and sound velocity profiles to the swaths; (2) editing of spurious navigation points; (3) application of beam number, depth, quality, nadir and statistic filters for every line; (4) manual editing of each line; and (5) construction of a Digital Terrain Model (DTM) with 50 m grid cell size.

Sub-bottom profiler data were plotted at OGS using the SEISPRO software developed at the Marine Science Institute (ISMAR) (Gasperini and Stanghellini 2005).

Results

The analysis of swath bathymetry data allowed identifying tens to hundreds meters in length small-scale morphologic features and larger submarine canyons, while the examination of sub-bottom profiles allowed the characterization of the internal seismic facies of those features. The morphological features are not evenly distributed in the study area, but are in most cases specific to a certain geographic sector. We provide in this chapter a description of the different morphologic features and of their geographic/physiographic setting.

Seafloor undulations with internal layered seismic facies

Seafloor undulations with an average wavelength of about 100 m and layered internal seismic facies have been identified in the Corigliano and Amendolara basins. We describe here those from the Corigliano Basin since the survey there extended to shallower depths, thus allowing a better definition of the relationships with inland and shelf elements. The sedimentary undulations occupy two along-slope elongated stripes of few hundreds of km^2 in total at ~400 m water depth where the seafloor gradient is 1–2°. The first N–S elongated strip in the northernmost part of the basin, between Capo Spulico and offshore Raganello stream (Figs. 1, 2), is about 10 × 5 km in size and ranges from ~350 to 450 m in depth. The second undulations field occurs in the northwesternmost part of the basin, on the margin segment between Crati and Trionto river mouths, and is NNW-SSE oriented. Its area is ~20 × 10 km within a depth range of 400–500 m.

The undulations have rounded crests and narrow troughs, do not show evidence of lateral migration, and have variable dimensions. The wavelength is ~100 m in average, ranging from several tens of meters to nearly 200 m. The undulations height generally is 1–5 m (Figs. 3, 4). The crests are most often sinuous and only occasionally straight or bifurcated. Since the length of the bifurcating crests is often comparable to the length of the associated crest, it is unclear if they actually correspond to single undulations that bifurcate or if they simply are converging crests disposed at an angle, which is usually close to 30°. Lateral terminations of the crests are generally aligned with troughs located between the crests of contiguous undulations or with bifurcations of the contiguous undulations. The lateral continuity of the undulations generally ranges from some hundreds of m to about 1 km. The recurrence in the configuration (straight versus curved, or sinuous or bifurcated) and orientation of the undulations is generally low. Normally less than ten consecutive undulations have the same orientation or configuration. The observed high variability in configuration and the low lateral continuity of the undulations rends somehow difficult determining their mean trend, which varies between NNW-SSE and NNE-SSW. In general the orientation of the undulations appears to be sub-parallel to the local bathymetric contours: N–S in the northernmost strip between Capo Spulico and the Raganello mouth (Fig. 3) and more variable, from NNE-SSW to NNW-SSE, in the northwestern strip between the Crati and Trionto river mouths (Fig. 4).

The sub-bottom profiles within the two fields of seafloor undulations within the Corigliano Basin show a well-

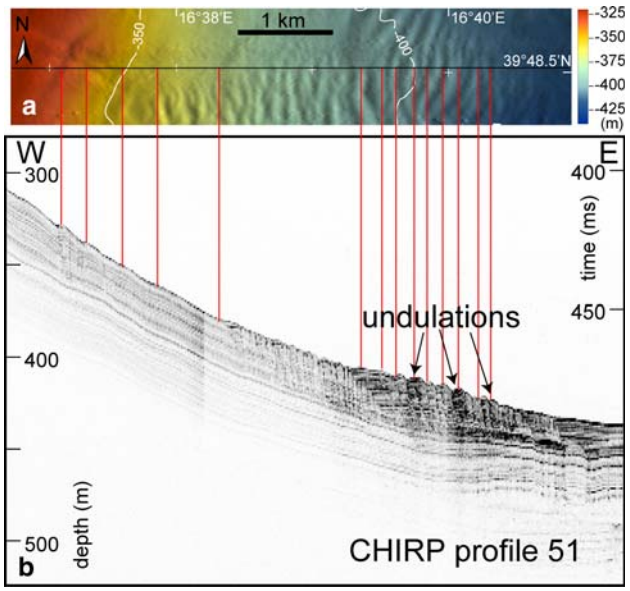

Fig. 3 Seafloor undulations with internal layered facies. (**a**) Shaded relief bathymetry map. Grid spacing = 20 m; vertical factor = 8; illumination from 280°; contour interval = 50 m. Location in Fig. 2. (**b**) Chirp profile 51 crossing perpendicularly the seafloor undulations. Location in Fig. 3a

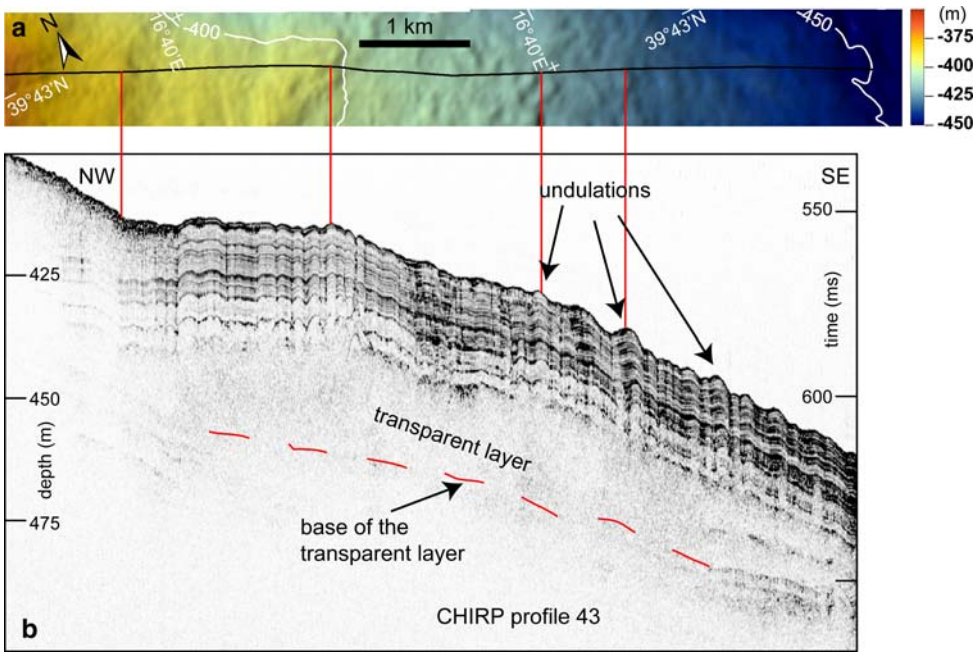

Fig. 4 Seafloor undulations with internal layered facies. (**a**) Shaded relief bathymetry map. Grid spacing = 25 m; vertical factor = 10; illumination from 330°; contour interval = 50 m. Location in Fig. 2. (**b**) Chirp profile 45 obliquely crossing the seafloor undulations. Location in Fig. 4a

layered seismic facies with undulated, conformable reflectors. The penetration appears to be generally low (between 20 and 40 ms) and in any case lower than observed elsewhere by similar layered facies within the western Gulf of Taranto. A more careful examination of the profiles unveils a rough upward convex transparent to chaotic seismic unit below the layered facies (Figs. 3, 4). The overlying stratified parallel reflectors up to the seafloor conformably match the roughness of the upper surface of the underlying transparent/chaotic unit. Applying the principle of normal upward causal relationship (i.e. overlying morphology is generally inherited from the underlying one) the conformable nature of the overlying layered facies indicates that the undulations were generated by the underlying (pre-existent) unit or that both units have been simultaneously modified after deposition. Artefacts and/or sea-surface wave effects causing the observed undulations are excluded since they would have affected sub-bottom profiles along all their length, whereas parts of the profiles appear undulation free.

Seafloor undulations with internal opaque seismic facies

A completely different kind of seafloor undulations characterized by an internal opaque seismic facies with no internal reflectors has been identified on the upper continental slope of the Calabrian margin, in front of the Trionto river mouth (Figs. 1, 5). We name this facies "opaque" as there is an absolute lack of reflections below the seafloor. These undulations occur between ~400 and 500 m depth, within a ~2 × 3 km fan-shaped depressed area at the mouth of a relatively large gully (Fig. 5) where, following Damuth's (1980) terminology, a prolonged and continuous high-amplitude echo characterizes the seafloor. The undulations arrangement is roughly concentric around a nucleus close to the apex of the fan-shaped area at ~400 m depth. The seafloor gradient is 2–3°. The undulation wavelength is ~500 m, with a maximum amplitude of 10 m. At least five of these seismically opaque undulations exist. These undulations seem to be unique, as they have not been detected associated to the other gullies, of comparable width, present in this sector of the margin. Additional morphologic features visible within the same gully include crescent-like undulations in the upper part and meanders in the lower part, in between the crescents and the concentric undulations. The seismic facies in the area adjacent to the undulations is layered with conformable reflectors. Those layered sediments onlap the underlying opaque facies with undulated top, as shown in Fig. 5.

Seafloor sub-parallel linear depressions

Numerous NW-SE oriented sub-parallel linear depressions occupy a few square km roughly rectangular area on the continental shelf and upper slope of the westernmost Corigliano Basin, where they extend from 50 to 350 m of water depth (Fig. 6). The length of the linear depressions, which are almost normal to the local NE-SW trending contours, is from 1 to 10 km while their spacing is generally between 150 and 200 m. The incision depth of the depressions is always less than 2 m.

Sub-bottom profiles show that the seafloor linear depressions correspond to downward bends of the bottom

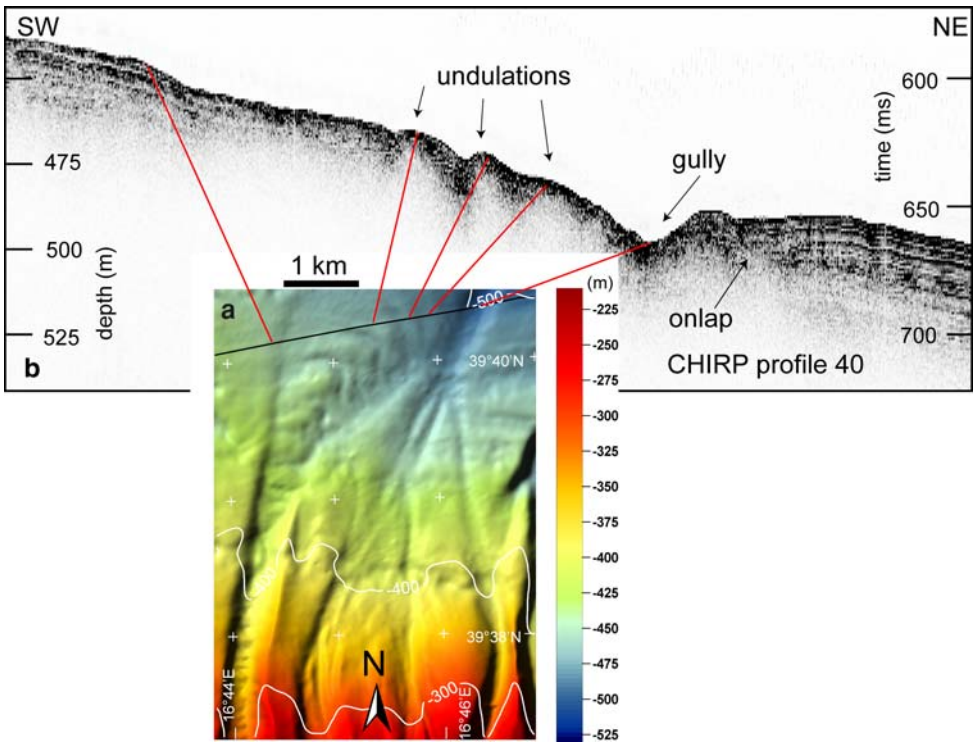

Fig. 5 Seafloor undulations with internal opaque acoustic facies. (**a**) Shaded relief bathymetry map. Grid spacing = 20 m; vertical factor = 8; illumination from 320°; contour interval = 100 m. Location in Fig. 2. (**b**) Chirp profile 40 obliquely crossing the seafloor undulations. Location in Fig. 5a

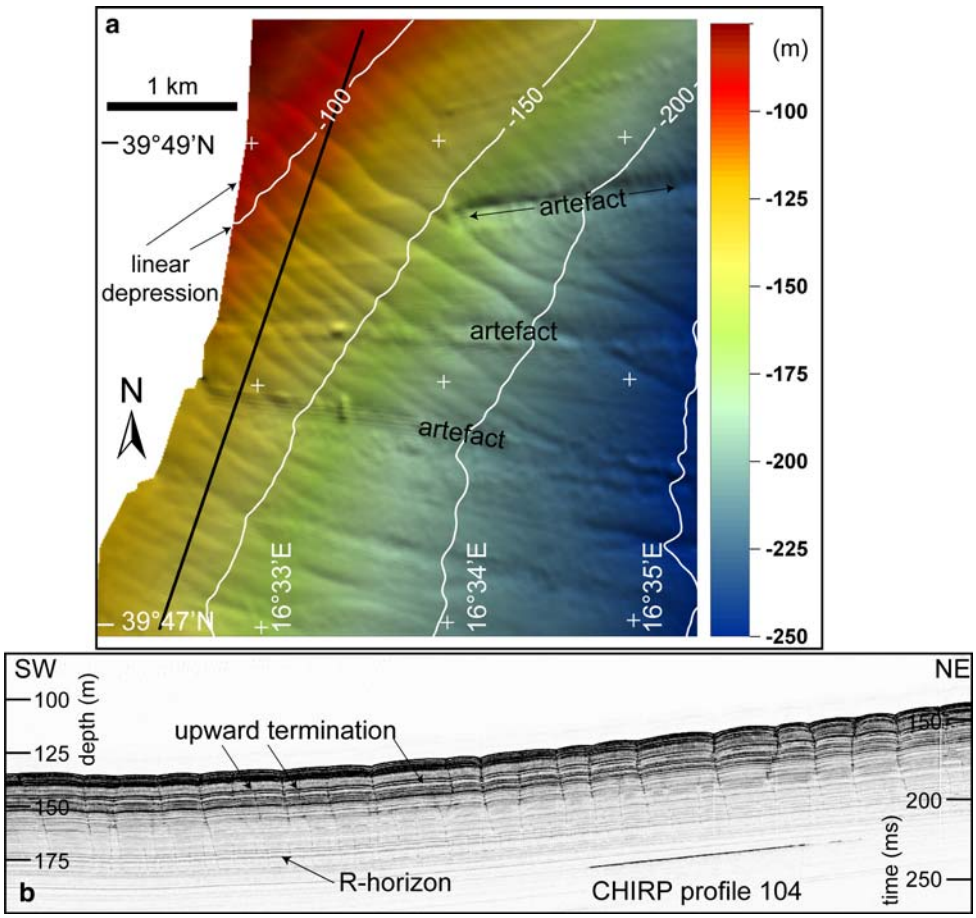

Fig. 6 Dip-slope elongated linear depressions. (**a**) Shaded relief bathymetry map. Grid spacing = 10 m; vertical factor = 5; illumination from 25°; contour interval = 50 m. Location in Fig. 2. (**b**) Chirp profile 104 orthogonal to the linear depressions in their proximal part. Location in Fig. 6a

reflector (Fig. 6b). The internal seismic facies is well stratified, and consists of closely packed sub-horizontal conformable reflectors. A sub-vertical reflection crossing the sub-horizontal reflectors appears in correspondence to every seafloor depression (Fig. 6b). A closer look to the sub-bottom profiles reveals that a piling up of paleo-depressions generates each sub-vertical reflection, and that the continuous sub-horizontal reflectors also bend downwards conformably to the seafloor. However, little or no vertical offset is observed at the location of the sub-vertical reflections. The sub-vertical reflections appear because the central points of the sub-vertically piled paleo-depressions look darker than the rest of the corresponding reflectors due to focusing of seismic energy within concavities. Most of these sub-vertical reflections looking as discontinuities affect a sediment thickness of about 50 ms (nearly 40 m) down to the previously mentioned R horizon (Fig. 6b) identified by Romagnoli and Gabbianelli (1990). However, some of these reflections are shallower, terminating few meters below the seafloor before reaching the R horizon.

Lens-shaped transparent deposits

Lens-shaped transparent deposits have been identified in the upper part of the sedimentary infill of the tectonically controlled Amendolara Basin (Fig. 2). The transparent deposits, which are clearly visible in the sub-bottom profiles, do not have a distinctive morphologic expression on the multibeam bathymetry images. The swath bathymetry data have been nevertheless helpful, when analyzed in conjunction with sub-bottom profiles, to estimate the extension of the transparent deposits (Fig. 2). These deposits, bounded at their basis and top by packages of undisturbed continuous reflectors, are unquestionably just above the R horizon of Romagnoli and Gabbianelli (1990) (Fig. 7a).

The northernmost transparent deposit covers about 25 km^2 (transparent deposit 2 in Fig. 2), is 25 ms ($\sim$20 m) thick and completely lacks internal reflectors (Fig. 7a). It has an estimated volume of $\sim$0.5 km^3. The second transparent deposit (transparent deposit 1 in Fig. 2) lies within a depression at nearly 1,000 m depth in the eastern part of the Amendolara Basin. The deposit occupies an area of $\sim$100 km^2, is up to 40 ms (about 30 m) thick and involves a sediment volume of $\sim$3 km^3 (Fig. 7a).

At shallower depths to the east and northeast of the transparent deposits described in the previous paragraph there is a reflection-lacking facies that looks very similar to that of the lens-shaped transparent deposits. This facies is capped by about 20 ms ($\sim$15 m) of seismically stratified sediments and extends deeper than the lower limit of penetration of our sub-bottom profiles, which suggests a considerable thickness. The area of this deposit is possibly $\sim$100 km^2 though it has not been mapped in Fig. 2 since its lateral limits have not been detected. This transparent deposit thins towards the structural heights of the Amendolara Ridge. It is to be noticed that the acoustic signal within the stratified sediments overlying the transparent layer is locally lost because of acoustic wipeouts, which may suggest the presence of gas in the sediments (Fig. 7b).

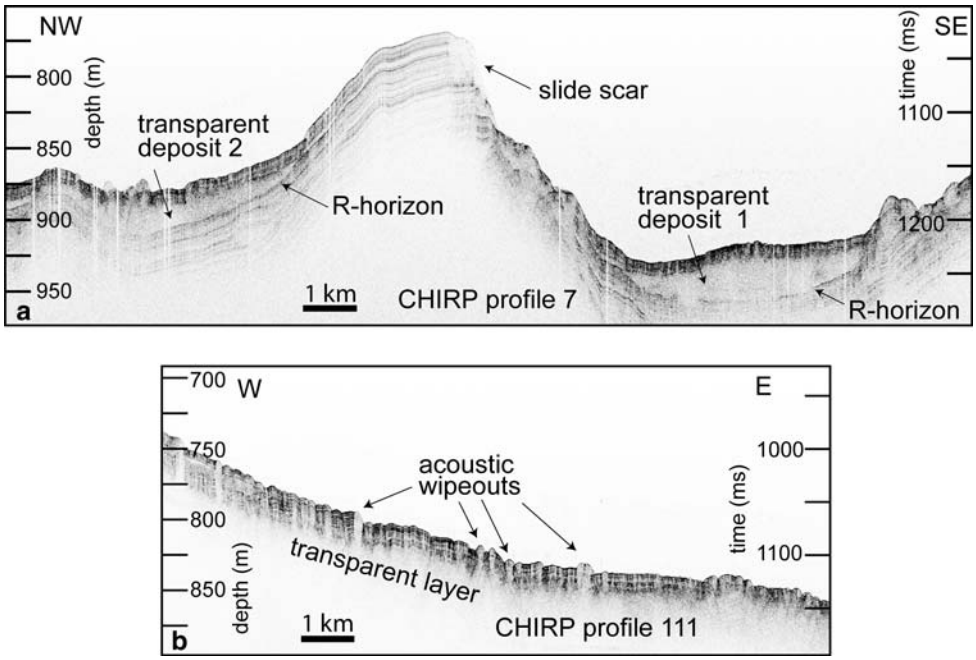

Fig. 7 Chirp profiles in the Amendolara Basin. Location in Fig. 2. (**a**) Chirp profile 7 in the central part of the basin, crossing two transparent deposits mapped in Fig. 2. (**b**) Chirp profile 111 in the western part of the basin, crossing a poorly constrained transparent deposit (not mapped in Fig. 2) overlain by undulations with acoustically layered facies showing acoustic wipeouts

Landslide scars

No major scars have been identified with confidence in the study area. Only relatively small scars, about 500 m wide, have been detected on the southern flank of the Amendolara Basin, over the ESE oriented extension of Amendolara Ridge, at about 500 m of water depth (Fig. 8). These SW-NE elongated, spoon-shaped scars are a few tens of meters in relief only. Further landslide scars are visible on the flanks of the Neto-Lipuda Canyon (see next section). The search for additional small landslide scars in other zones of the study area would require a systematic and rigorous examination of the whole data set, a task that we have not performed in full as it goes beyond the scope of the present work.

Neto-Lipuda and Alice canyon systems

The Neto-Lipuda Canyon is fed by the Neto and Lipuda rivers (Fig. 1). Our dataset covers the upper half of the course of the E-W trending Neto-Lipuda Canyon down to about 35 km from the shelf margin. Neto and Lipuda rivers feed the 24 km wide, amphitheatre-shaped canyon head (Figs. 1, 2). The fresh-looking appearance of the canyon head and its tributary minor canyons suggests that it is an active feature retrogressively eroding the upper slope and shelf (Fig. 9a). Three V-shaped main tributary canyons are identified on the upper slope, which are a SSW-NNE trending southern canyon originating off the mouth of the Neto River, a NW-SE trending northern canyon originating off the mouth of the Lipuda River, and a shorter NW-SE trending intermediate canyon resulting from the convergence of two short E-W trending valleys located in between the mouths of Neto and Lipuda rivers (Fig. 9a). These three tributary canyons converge into the Neto-Lipuda Canyon at about 1,100 m depth. After the confluence the canyon becomes flat-bottomed (Fig. 9b) and runs towards the ENE for about 10 km before forming a marked meander (Fig. 2).

A prolonged bottom echo characterizes canyon floors and no reflectors are identified within the underlying opaque seismic facies (Fig. 9). Perched acoustically transparent sediment lenses are visible on the terraces to the north and south of the Neto-Lipuda Canyon. These transparent lenses are bounded at their base and top by packages of laterally continuous sub-parallel reflectors (Fig. 9b). The northern largest lens-shaped deposit is at least 3 km long and up to ~25 ms (~20 m) thick. Despite their limited resolution, the multibeam data show some features on the flanks of the Neto-Lipuda Canyon meander that could be interpreted as landslide scars (Figs. 2, 10). The largest, sub-circular scar is about 2 km wide and has a relief of about 100 m (Fig. 10).

The NW-SE trending, long, meandering Alice Canyon originates on the inner continental shelf offshore Punta Alice and does not seem to be related to any river mouth (Figs. 1, 2). Its path is sub-parallel to the upper course of the Neto-Lipuda Canyon. The course of the Alice Canyon within the surveyed area shows six prominent meanders, of which the most well-defined is in correspondence to the Cirò Ridge and to a smaller NW-SE ridge immediately to the south (Fig. 2). The canyon is V-shaped in cross-section and has an average width of less than 1 km along the

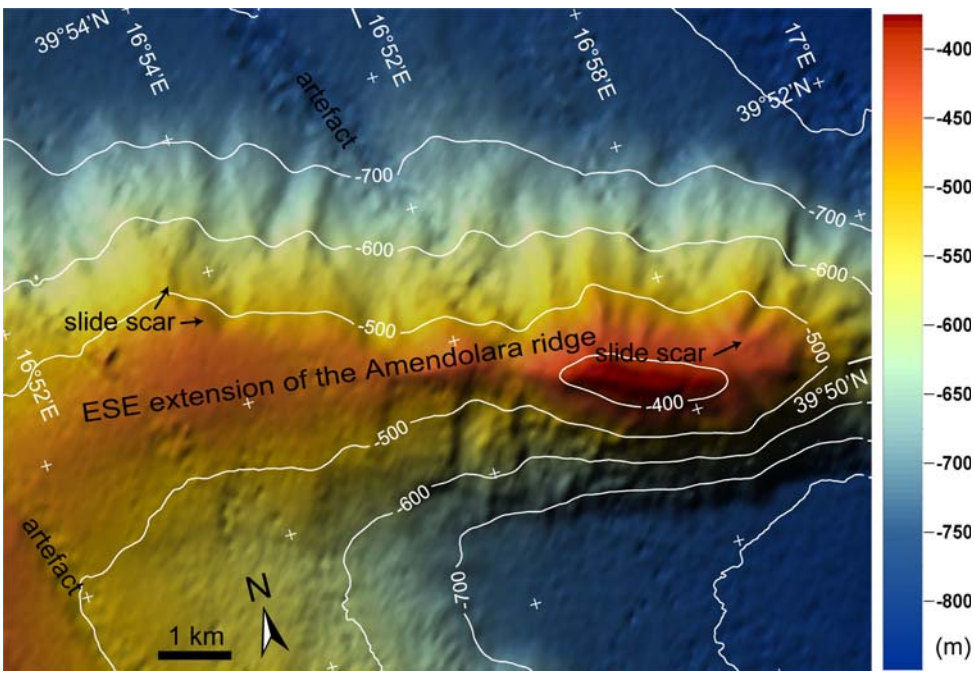

Fig. 8 *Shaded* relief bathymetry map showing slide scars on the northern flank of the Amendolara Ridge. Grid spacing = 50 m; vertical factor = 3; illumination from 300°; contour interval = 100 m. Location in Fig. 2

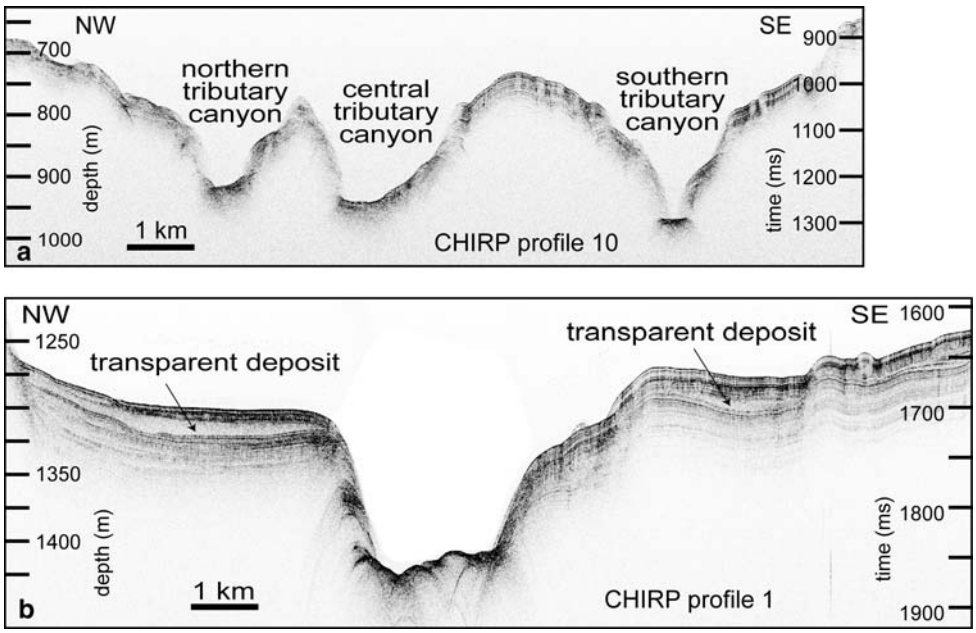

Fig. 9 Strike chirp profiles crossing the Neto-Lipuda canyon system. Location in Fig. 2. (**a**) Chirp profile 10 crossing the V-shaped tributary canyons in the upper part of the system. (**b**) Chirp profile 1 in central part of the system, crossing the U-shaped Neto-Lipuda canyon and lensoidal transparent facies on the flanks

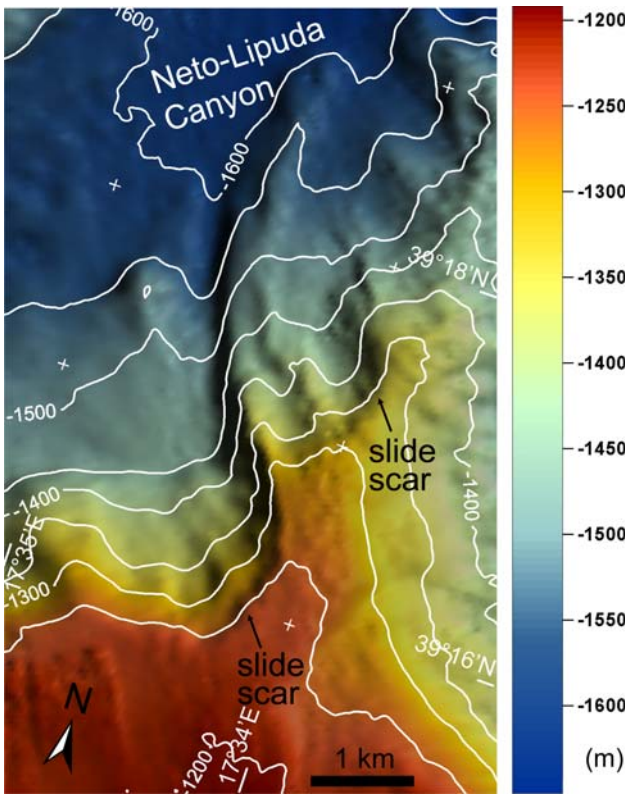

Fig. 10 *Shaded* relief bathymetry map showing slide scars on the northern flank of the distal part of the Neto-Lipuda canyon. Grid spacing = 50 m; vertical factor = 3; illumination from 70°; contour interval = 50 m. Location in Fig. 2

~30 km of surveyed upper course. Unlike Neto-Lipuda Canyon, no appreciable landslide scars have been identified on the flanks of Alice Canyon.

Discussion

Seafloor undulations with internal layered seismic facies

The interpretation of the seafloor and sub-seafloor undulations with internal layered seismic facies observed in the Corigliano and Amendolara basins is not straightforward. Several options about their genesis have to be considered at the light of studies on similar features made elsewhere (e.g. Faugères et al. 2002; Cattaneo et al. 2004; Marsset et al. 2004; Fernández-Salas et al. 2007).

A plausible interpretation would relate the observed undulations to slow sediment deformation processes such as sediment creep, which has been evoked for similar seafloor features (Correggiari et al. 2001; Lykousis et al. 2003; Alonso et al. 1995). In fact, Romagnoli and Gabbianelli (1990) already interpreted the seafloor undulations in the Corigliano Basin as creep folds produced by slow plastic deformation under a continuous load (Hill et al. 1982). These authors cored these features of late Pleistocene–Holocene age and interpreted them as the result of shallow deformation, clearly distinguishing them from the sediment waves produced by turbidity currents. However, the slope angle of the Calabrian margin of the Corigliano Basin is quite low, about 1° and in any case lower than 2°. This poses some difficulties to the development of creep folds. In addition, the shape of the undulations quite perfectly matches the top roughness of the underlying transparent unit (Figs. 4, 7b). This evidence is hardly explained by the creep fold hypothesis and is generally viewed as an evidence for a depositional origin with

sediment undulations developing on pre-existing seafloor roughness (e.g. Cattaneo et al. 2004).

The hypothesis that the observed undulations are sediment waves produced solely by depositional processes cannot be totally ruled out, but does not seem very likely. The observed undulations do not fit well into the category of sediment waves generated by along-slope (contour) currents (Wynn and Stow 2002). In fact, the observed undulations are sub-parallel to the contours, whereas sediment waves generated by along-slope currents are usually perpendicular or oblique to flow direction and hence to the contours (e.g. Verdicchio and Trincardi 2006; Hanquiez et al. 2007).

The observed undulations could be interpreted as generated by spillover or overbanking processes, or by flow stripping of turbidity currents (Normark et al. 1980, 2002) feeding the Crati submarine fan (Ricci Lucchi et al. 1984; Colella and Normark 1984). An alternate option is considering these undulations as produced by river-sourced hyperpycnal flows, similarly to the interpretations made in other areas (Urgeles et al. 2007; Bornhold and Prior 1990; Yoo et al. 2002; Mulder and Syvitski 1995). The undulations of the study area display an along-slope trend that is compatible with their interpretation as the product of hyperpycnal flows. Furthermore, several Apennine Rivers are likely to develop hyperpycnal discharges (Khan et al. 2005). However, differently from most undulations produced by turbidity currents and hyperpycnal flows, the observed undulations are apparently standing with no evident signs of migration, change their wavelength from one to another without any appreciable trend, and are unrelated to erosional features. In fact, some lateral migration, generally upslope, and distinct size trends, usually with downslope decrease in size have been commonly observed in sediment waves reported elsewhere (Wynn and Stow 2002). Moreover, sediment waves are frequently associated to erosional features (Verdicchio and Trincardi 2006; Fernández-Salas et al. 2007; Wynn and Stow 2002). All these differences do not support the interpretation of the observed undulations as sediment waves. However, such an origin cannot be definitively excluded.

The observed undulations are hence interpreted as resulting from a combination of processes, including soft-sediment deformation (creeping) and sediment deposition by downslope density (hyperpycnal) flows. Such deposition would essentially drape the underlying transparent deposits, whose roughness is matched to a large extent by the observed undulations.

Slope and canyon flank instabilities

Evidences of sliding along the steep and tectonically active flanks of the Amendolara Ridge were previously recognized and described by Romagnoli and Gabbianelli (1990) based on sub-bottom profiler data. Slide scars have been also identified in our data set on the steep edges of the Amendolara Ridge (Fig. 8) and on the southern flank of the Neto-Lipuda Canyon (Fig. 10). Mulder and Cochonat (1996) defined slides and slumps as movements of coherent masses of sediment bounded by distinct failure plans. Slide triggering has been attributed to the presence of gas into the sediment, earthquake shaking, sediment loading and different combinations of other destabilisation factors (e.g. Canals et al. 2004 and references therein). Earthquake related triggering mechanisms include loading by horizontal and vertical accelerations, liquefaction and fault rupture induced sliding (e.g. Canals et al. 2004 and references therein).

The location of slide scars in the study area on the flanks of the tectonically controlled Amendolara Ridge points to tectonic activity as the potential main trigger, possibly by earthquake fault rupture induced sliding. This view is supported by the intense seismic activity occurring at the Calabrian margin (Caputo et al. 1972; Brogan et al. 1975; Gasparini et al. 1982). The neotectonic regime in northern Calabria is characterized by an ESE-WNW oriented tensile axis (Cello et al. 1982). The scattered distribution of intermediate and deep focus earthquakes and fault plane solutions imply regional uplift accompanied by strike-slip mechanisms (Riuscetti and Schick 1975; Brogan et al. 1975).

However, we have not been able to precisely locate on the sub-bottom profiles the slide deposits issued from the Amendolara Ridge scars. These deposits are possibly buried by younger sediments and lay beneath the maximum penetration depth of our sub-bottom profiles. An alternate view is that the slides evolved into debris flows while moving down towards the Amendolara Basin. Supporting this hypothesis are the lens-shaped, acoustically transparent deposits previously described and interpreted as mass flow deposits (Ricci Lucchi et al. 1984; Colella and Normark 1984 (Figs. 2, 7).

Submarine erosion is known to play a major role in canyon development as well as mass wasting of canyon walls and retrogressive sediment failure in canyon's head (Lastras et al. 2007; van Weering and Weaver 2007 and references therein). In the case of the Neto-Lipuda Canyon, we infer that a complex combination of erosive turbidity and hyperpycnal currents jointly with slides, slumps and debris flows are the main cause of the most relevant morphologic features. The canyon head and the upper course V-shaped cross-section (Figs. 2, 9a) suggest active erosion possibly due to the action of river sourced hyperpycnal flows and turbidity currents directly feeding the various branches forming the canyon head. The down course U-shaped geometry of the Neto-Lipuda Canyon (Fig. 9b),

together with the scars observed on its flanks (Fig. 10), suggest that canyon evolution there is controlled by side-wall collapse leading to progressive infilling of the valley floor.

Up course sliding also occurs on the sides of the branching tributaries that converge into the main canyon. The small volume resulting slide deposits accumulating on the base of valley walls and on valley floors lie above the equilibrium baseline of the canyon axis and, therefore, are easily washed and eroded by subsequently turbidity currents and hyperpycnal flows.

Alice Canyon displays a V-shaped cross-section all along the investigated reach, which indicates that the main factor controlling its evolution is erosional processes. In that canyon sliding might play a secondary role.

Debris flow and other plastic flow deposits

The seismically transparent facies observed in the Amendolara (Fig. 7) and Corigliano (Figs. 3, 4) basins and on the flanks of the Neto-Lipuda Canyon (Fig. 10) markedly contrasts with the continuous stratified facies characteristic of undisturbed slope deposits. We interpreted the transparent units as debris flow deposits.

A debris flow is a mass movement involving rapid flowage of rock debris of various kinds under various conditions, specifically a high-density mudflow containing abundant coarse-grained materials (Bates and Jackson 1987). In both debris and plastic flows, gravity is an important factor for motion, while for other type of mass flows the motion is mainly due to the presence of interstitial fluid (Mulder and Cochonat 1996).

In the Amendolara Basin (Fig. 7), the debris flow deposits are located above the R horizon of Romagnoli and Gabbianelli (1990). The reflectors below the debris flow deposits are undisturbed, while the overlying sediment layers locally show hyperbolic reflections that may indicate fluid escape as previously inferred by Romagnoli and Gabbianelli (1990).

The seafloor undulations on the upper Calabrian continental slope in front of the Trionto River (Fig. 5) differ from those identified elsewhere in the study area (Figs. 3, 4, 7b) since their internal seismic facies is not stratified but more similar to the facies of the debris flow deposits found in the Corigliano and Amendolara basins (Figs. 3, 4, 7a) and on the flanks of the Neto-Lipuda Canyon (Fig. 9b). Most of the debris flow deposits found in those areas have a rough undulated upper surface that does not outcrop as it is overlain by younger stratified sediments. It is likely that the seafloor undulations off the Trionto River mouth also correspond to the top or upper part of a debris flow deposit. The fact that this specific deposit is not buried is attributed to its location in an area of predominant sediment bypass as indicated by the large upper slope gully opening exactly off the river mouth. It must be noted again that the opaque facies outcrops in a depressed area and is laterally on lapped by stratified sediments (Fig. 5). The interpretation of this opaque facies as a debris flow deposit is further supported by the concentric disposal of the undulations as they appear on the seafloor, which suggest a plastic behavior. According to Mulder and Cochonat (1996), plastic flows usually result from the movement of under consolidated masses of sediments. The mass movement category of plastic flows includes debris flow and mud flows (Canals et al. 2004). As we do not have elements to ascribe the internally opaque undulations to a specific type of plastic flow we prefer to use the generic term “plastic flow deposits”. Within this uncertainty it seems likely that the plastic behavior evidenced by the seafloor concentric undulations involved predominantly fine-grained sediment with some degree of fluidity during motion. However, it cannot be totally ruled out that the detection of reflectors below this type of undulations is prevented by a seafloor coarse-grained lag resulting from deposition after turbidity currents flowing down the above mentioned large gully.

The setting of the area where the opaque undulations have been found provides a good explanation for the occurrence of plastic flows. First, there is a high sediment supply by the Trionto River and the numerous torrential streams opening into the sea (Romagnoli and Gabbianelli 1990) leading, for instance, to a sedimentation rate of 6 mm/yr in the Corigliano Basin. Second, the frequent earthquakes inherent to the tectonically active southern Italy foreland basin contribute the external loading required to trigger the flows (Caputo et al. 1972; Brogan et al. 1975).

Seafloor sub-parallel linear depressions

The linear depressions in the westernmost Corigliano Basin are not easy to interpret. Solely using sub-bottom seismic profiles, Romagnoli and Gabbianelli (1990) interpreted these linear depressions as creep folds sliding on the R horizon and the larger ones as pockmarks. However, the new multibeam data here presented show that the linear depressions are almost orthogonal to the bathymetric contours (Fig. 6a). This evidence discards these linear depressions being interpreted as creep folds, which would be sub-parallel to the slope, or as pockmarks, which would not be necessarily aligned. The new data also rule out a possible interpretation as polygonal faults similar to those identified, for instance, by Cartwright and Dewhurst (1998).

We notice that the orientation of the linear depressions is sub-parallel to onshore transpressive structures such as

the Rossano-S. Nicola and Pollino fault systems, and that many of the depressions are rooted in the R horizon (Fig. 6b). Following Romagnoli and Gabbianelli (1990) the R horizon might represent a change in the rheologic behavior of the sediments and hence a transfer surface for subsequent tectonic movements. Therefore, the linear depressions could be the expression of minor shallow faults (P and R shears) associated to a major fault system, which lies below the R horizon and is not detected in our data set. Similar *en-èchelon* associations of small faults at small angles to the main fault have been documented elsewhere as the surface expression of deeper strike-slip faults (Christie-Blick and Biddle 1985 and references therein; Sylvester 1988).

An alternative interpretation is that the linear depressions that are orthogonal to the contours result from incision by downslope sediment-laden flows. However, the Crati River, which would be the source of such flows, is located nearly 10 km to the south of the linear depressions shown in Fig. 6a. Moreover, the very narrow character of the incisions would suggest quite an ephemeral nature of the density flows, which is in contrast with the relatively regular vertical alignment of the depressions (Fig. 6b).

Summary and conclusions

The integrated analysis of new multibeam bathymetry and seismic sub-bottom data has brought to light mass wasting features and soft-sediment deformation in the western Gulf of Taranto, which belongs to the southern Italy foreland basin system. The features identified include:

(i) Slides and slide scars, visible mostly on the relatively steep flanks of the Amendolara Ridge and in the Neto-Lipuda Canyon system. In the latter, the slides contribute, along with turbidity currents and debris flows, to the evolution of the canyon system, marked by retrogressive erosion of the canyon head and progressive infilling of the deeper canyon floor. Widely distributed debris flow deposits of variable size have been identified based on their transparent seismic facies and upward convex lensoidal geometry.

(ii) Undulations affecting the superficial sediments of the Corigliano and Amendolara basins are interpreted as the result of a number of processes including soft-sediment deformation (creeping) and sediment deposition by downslope density (hyperpycnal) flows. We infer that their rough undulated character directly relates to the roughness of the underlying mass wasting deposits.

(iii) Seafloor linear depressions associated to subvertical reflections produced by the vertical piling up of buried depressions pose some interpretation difficulties. Their linear trend normal to the contours is against previous interpretations as creep folds and pockmarks, and is not in favor of polygonal faults. From the available data we consider that a more sound explanation is that these linear depressions may represent either secondary shallow faults or result from erosion by downslope flows.

Among the plausible preconditioning factors (Canals et al. 2004) for the identified mass wasting processes, the high sedimentation rates in the study area likely are the most significant, with numerous rivers and torrents responding for such high sediment input. The presence of fluids (gas and/or water) within the sediment cover that may also contribute to sediment destabilization is suggested by acoustic wipeouts in sub-bottom profiles. Finally, the frequent seismic shaking of the area is the most likely triggering factor for mass wasting events.

Acknowledgments The dataset on which this paper is built was acquired during the WGDT cruise (P.I. Salvatore Critelli, University of Calabria) on board OGS-Explora, supported with OGS institutional funds. Data processing has been performed within GEMAR and PROS groups from OGS. The authors acknowledge the support given by the shipboard party of R/V OGS Explora. We thank the referees Antonio Cattaneo, Galderic Lastras and Ruth Duran and guest editor Miquel Canals for their thoroughly review and helpful suggestions. NRC would like to thank the EC-FPV Research and Training Network EURODOM (European Deep Ocean Margins) for partially funding this research study and Danilo Morelli for constructive comments.

References

Alonso B, Canals M, Palanques A, Rehault JP (1995) A deep-sea channel in the northwestern Mediterranean Sea: morphology and seismic structure of the Valencia Channel and its surroundings. Mar Geoph Res 17:469–484

Bates RL, Jackson JA (1987) Glossary of geology, 3rd edn. American Geological Institute, Alexandria, Virginia, p 788

Boccaletti M, Nicolich R, Tortorici L (1984) The Calabrian Arc and the Ionian Sea in the dynamic evolution of the Central Mediterranean. Mar Geol 55:219–245

Bornhold BD, Prior DB (1990) Morphology and sedimentary processes on the subaqueous Noeick River delta, British Columbia, Canada. In: Colella A, Prior DB (eds) Coarse-grained deltas. Spec Publ Int Assoc Sedimentol 10, pp 169–184

Bousquet JC (1973) La tectonique recente de l'apennin calabro lucanien dans son cadre geologique et geophysique. Geol Rom 12:1–104

Brogan GE, Cluff LS, Taylor CL (1975) Seismicity and uplift of southern Italy. Tectonophysics 29:323–330

Canals M, Lastras G, Urgeles R, Casamor JL, Mienert J, Cattaneo A, De Batist M, Haflidason H, Imbo Y, Laberg JS, Locat J, Long D, Longva O, Masson DG, Sultan N, Trincardi F, Bryn P (2004) Slope failure dynamics and impacts from seafloor and shallow sub-seafloor geophysical data: case studies from the COSTA project. Mar Geol 213:9–72

Caputo M, Panza GF, Postpischl D (1972) New evidences about the deep structure of the Lipari Arc. Tectonophysics 15:219–231
Cartwright JA, Dewhurst DN (1998) Layer-bound compaction faults in fine grained sediments. Geol Soc Am Bull 110:1242–1257
Cattaneo A, Correggiari A, Marsset T, Thomas Y, Marsset B Trincardi F (2004) Seafloor undulation pattern on the Adriatic shelf and comparison to deep-water sediment waves. Mar Geol 213:121–148
Cello G, Guerra I, Tortorici L, Turco E, Scarpa R (1982) Geometry of the neotectonic stress field in southern Italy: geological and seismological evidence. J Struct Geol 4:385–393
Christie-Blick N, Biddle KT (1985) Deformation and basin formation along strike-slip faults. In: Biddle KT, Christie-Blick N (eds) Strike-slip deformation, basin formation, and sedimentation, SEPM Special Publication 37: pp 1–34
Colella A, Normark WR (1984) High-resolution side-scanning sonar survey of delta slope and inner fan channels of Crati submarine fan (Ionian Sea). Mem Soc Geol It 27:381–390
Correggiari A, Trincardi F, Langone L, Roveri M (2001) Styles of failure in late Holocene highstand prodelta wedges on the Adriatic shelf. J Sediment Res 71:218–236
Critelli S (1999) The interplay of lithospheric flexure and thrust accommodation in forming stratigraphic sequences of the southern Apennines foreland basin system. Accademia Nazionale dei Lincei, Rendiconti di Scienze Fisiche 10:257–326
Critelli S, Le Pera E (1998) Post-oligocene sediment dispersal systems and unroofing history of the Calabrian microplate, Italy. Int Geol Rev 40:609–637
Damuth JE (1980) Use of high-frequency (3.5–12 kHz) echograms in the study of near-bottom sedimentation processes in the deep-sea: a review. Mar Geol 38:51–75
DeCelles PG, Giles KA (1996) Foreland basin systems. Basin Res 8:105–123
Del Ben A (1993) Calabrian Arc tectonics from seismic exploration. Boll Geof Teor ed Appl 35:339–347
Doglioni C, Merlini S, Cantarella G (1999) Foredeep geometries at the front of the Apennines in the Ionian Sea (central Mediterranean). Earth Planet Sci Lett 168:243–254
Faugères JC, Gonthier E, Mulder T, Kenyon N, Cirac P, Griboulard R, Berne S, Lesuavé R (2002) Multi-process generated sediment waves on the Landes Plateau (Bay of Biscay, North Atlantic). Mar Geol 182:279–302
Fernández-Salas LM, Lobo FJ, Sanz JL, Díaz-del-Río V, García MC, Moreno I (2007) Morphometric analysis and genetic implications of pro-deltaic sea-floor undulations in the northern Alboran Sea margin, western Mediterranean Basin. Mar Geol 243:31–56
Ferranti L, Santoro E, Mazzella ME, Monaco C, Morelli D (2008) Active transpression in the northern Calabria Apennines, southern Italy. Tectonophysics. doi: 10.1016/j.tecto.2008.11.010
Finetti I (1976) Mediterranean ridge: a young submerged chain associated with the Hellenic Arc. Boll Geof Teor Appl 13(69):1–31
Gasparini C, Iannacone G, Scandone P, Scarpa R (1982) Seismotectonics of the Calabrian Arc. Tectonophysics 82:267–286
Gasperini L, Stanghellini G (2005) SEISPRO, a processing software for high resolution seismic data. ISMAR Technical Report 69
Hanquiez V, Mulder T, Lecroart P, Gonthier E, Marchès E, Voisset M (2007) High resolution seafloor images in the Gulf of Cadiz, Iberian margin. Mar Geol 246:42–59
Hill PR, Moran KM, Blasco SM (1982) Creep deformation of slope sediments in the Canadian Beaufort Sea. Geo Mar Lett 2:163–170
Khan SM, Imran J, Bradford S, Syvitski J (2005) Numerical modeling of hyperpycnal plume. Mar Geol 222–223:193–211
Lastras G, Canals M, Urgeles R, Amblas D, Ivanov M, Droz L, Dennielou B, Fabres J, Schoolmeester T, Akhmetzhanov A, Orange D, Garcia-Garcia A (2007) A walk down the Cap de Creus canyon, Northwestern Mediterranean Sea: Recent processes inferred from morphology and sediment bedforms. Mar Geol 246:176–192
Lykousis V, Sakellariou D, Rousakis G (2003) Prodelta slope stability and associated coastal hazards in tectonically active margins: Gulf of Corinth (NE Mediterranean). In: Locat J, Meinert J (eds) Submarine mass movements and their consequences, pp 433–440
Marsset T, Marsset B, Thomas Y, Cattaneo A, Thereau E, Trincardi F, Cochonat P (2004) Analysis of Holocene sedimentary features on the Adriatic shelf from 3D very high resolution seismic data (Triad survey). Mar Geol 213:73–89
Mulder T, Cochonat P (1996) Classification of offshore mass movements. J Sediment Res 66:43–57
Mulder T, Syvitski JPM (1995) Turbidity currents generated at river mouths during exceptional discharges to the world oceans. J Geol 103:285–299
Normark WR, Hess GR, Sow DAV, Bowen AJ (1980) Sediment waves on the Monterey Fan levee: a preliminary physical interpretation. Mar Geol 37:1–18
Normark WR, Piper DJW, Posamentier H, Pirmez C, Migeon S (2002) Variability in form and growth of sediment waves on turbidite channel levees. Mar Geol 192:23–58
Pennetta M (1992) Morfologia e sedimentazione della piattaforma continentale e scarpata nel tratto di costa compreso tra Punta Alice e Capo Rizzuto (Golfo di Taranto). Bol Soc Geol Ital 111:149–161
Pescatore T, Senatore MR (1986) A comparison between a present-day (Gulf of Taranto) and a Miocene (Irpinian Basin) foredeep of the Southern Apennines (Italy). IAS Spec Pub 8:169–182
Ricci Lucchi F, Colella A, Gabbianelli G, Rossi S, Normark WR (1984) The Crati Submarine Fan, Ionian Sea. Geo-Mar Lett 3:71–77
Riuscetti M, Schick R (1975) Earthquakes and tectonics in Southern Italy. Boll Geophys Teor Appl 27:59–77
Romagnoli C, Gabbianelli G (1990) Late quaternary sedimentation and soft-sediment deformation features in the Corigliano Basin, North Ionian Sea (Mediterranean). Giorn Geol 52(1–2):33–53
Rossi S, Gabbianelli G (1978) Geomorfologia del Golfo di Taranto. Boll Soc Geol It 97:423–437
Rossi S, Sartori R (1981) A seismic reflection study of the external Calabrian Arc in the N Ionian Sea (eastern Mediterranean). Mar Geoph Res 4:403–426
Rossi S, Auroux C, Mascle J (1983) The Gulf of Taranto (Southern Italy): seismic stratigraphy and shallow structure. Mar Geol 51:327–346
Senatore MR (1987) Caratteri sedimentari e tettonici di un bacino di avanfossa. Il golfo di Taranto. Mem Soc Geol It 38:177–204
Senatore MR, Normark WR, Pescatore T, Rossi S (1988) Structural framework of the Gulf of Taranto (Ionian Sea). Mem Soc Geol It 41:533–539
Sylvester AG (1988) Strike-slip faults. Geol Soc Am Bull 100:1666–1703
Urgeles R, DeMol B, Liquete C, Canals M, De Batist M, Hughes-Clarke JE, Amblàs D, Arnau PA, Calafat AM, Casamor JL, Centella V, De Rycker K, Fabrés J, Frigola J, Lafuerza S, Lastras G, Sànchez A, Zuñiga D, Versteeg W, Willmott V (2007) Sediments undulations on the Llobregat prodelta: Signs of early slope instability or sedimentary bedforms? J Geophys Res 112:B05102. doi:10.1029/2005JB003929
Van Dijk JP, Bello M, Brancaleoni GP, Cantarella G, Costa V, Frixa A, Golfetto F, Merlini S, Riva M, Torricelli S, Toscano C, Zerilli A (2000) A regional structural model for the northern sector of the Calabrian Arc (southern Italy). Tectonophysics 324:267–320
van Weering TCE, Weaver PPE (ed) (2007) EUROSTRATAFORM: role and functioning of Canyons. Mar Geol 246(2–4):247pp

Verdicchio G, Trincardi F (2006) Short-distance variability in slope bed-forms along the southwestern Adriatic margin (central Mediterranean). Mar Geol 234:271–292

Wynn RB, Stow AV (2002) Classification and characterisation of deep-water sediment waves. Mar Geol 192:7–22

Yoo DG, Lee CW, Kim SP, Jin JH, Kim JK, Han HC (2002) Late quaternary transgressive and highstand systems tracts in the northern East China Sea mid-shelf. Mar Geol 187:313–328